



Article

Numerical Simulation for a Hybrid Variable-Order Multi-Vaccination COVID-19 Mathematical Model

Nasser Sweilam ^{1,*},[†] , Seham M. Al-Mekhlafi ^{2,3},[†] , Reem G. Salama ⁴ and Tagreed A. Assiri ⁵

¹ Department of Mathematics, Faculty of Science, Cairo University, Giza 12613, Egypt

² Department of Mathematics, Faculty of Education, Sana'a University, Sana'a 1247, Yemen

³ Department of Engineering Mathematics and Physics, Future University in Egypt, New Cairo 11835, Egypt

⁴ Department of Mathematics, Faculty of Science, Beni-Suef University, Beni-Suef 62521, Egypt

⁵ Department of Mathematics, Faculty of Science, Umm Al-Qura University, Makkah 21961, Saudi Arabia

* Correspondence: nsweilam@sci.cu.edu.eg

[†] These authors contributed equally to this work.

Abstract: In this paper, a hybrid variable-order mathematical model for multi-vaccination COVID-19 is analyzed. The hybrid variable-order derivative is defined as a linear combination of the variable-order integral of Riemann–Liouville and the variable-order Caputo derivative. A symmetry parameter σ is presented in order to be consistent with the physical model problem. The existence, uniqueness, boundedness and positivity of the proposed model are given. Moreover, the stability of the proposed model is discussed. The theta finite difference method with the discretization of the hybrid variable-order operator is developed for solving numerically the model problem. This method can be explicit or fully implicit with a large stability region depending on values of the factor Θ . The convergence and stability analysis of the proposed method are proved. Moreover, the fourth order generalized Runge–Kutta method is also used to study the proposed model. Comparative studies and numerical examples are presented. We found that the proposed model is also more general than the model in the previous study; the results obtained by the proposed method are more stable than previous research in this area.

Keywords: variable-order hybrid operator; Pfizer vaccine; Moderna vaccine; Janssen vaccine; theta finite difference method; generalized fourth order Runge–Kutta method

MSC: 65L05; 37N30; 65M06



Citation: Sweilam, N.; Al-Mekhlafi, S.M.; Salama, R.G.; Assiri, T.A. Numerical Simulation for a Hybrid Variable-Order Multi-Vaccination COVID-19 Mathematical Model. *Symmetry* **2023**, *15*, 869. <https://doi.org/10.3390/sym15040869>

Academic Editors: Francisco Martínez González, Mohammed K. A. Kaabar and Juan Luis García Guirao

Received: 4 February 2023

Revised: 26 March 2023

Accepted: 30 March 2023

Published: 6 April 2023



Copyright: © 2023 by the authors. Licensee MDPI, Basel, Switzerland. This article is an open access article distributed under the terms and conditions of the Creative Commons Attribution (CC BY) license (<https://creativecommons.org/licenses/by/4.0/>).

1. Introduction

Coronaviruses are a large family of viruses known to cause illnesses ranging from the common cold to more serious illnesses such as severe acute respiratory syndrome [1]. The World Health Organization has designated this variant as a variant of serious concern. The United States Centers for Disease Control and Prevention has granted Emergency Use Authorization to the following vaccines: Pfizer-BioNTech with 95% efficacy against symptomatic COVID-19, Moderna vaccine with 94.5% efficacy and Janssen vaccine manufactured by Johnson & Johnson, which has an efficacy rating of 67%, as well as many others [1,2]. SARS-CoV-2 vaccinations have been shown to be effective against infections, including both silent and symptomatic cases, of severe COVID-19 illness and deaths [2]. Mathematical modeling is a valuable tool to study disease spread and control very effectively. Several mathematical models have been proposed in the literature to study and understand the novel complex transmission pattern of the COVID-19 pandemic; see, for example, [3–8].

In the meantime, there are now extensive articles explaining the advantage of fractional order models for studying real mathematical models in various fields [9]. The variable-order fractional derivatives (VOFDs) can describe the effects of the long variable memory of a time-dependent system. In [10], Samko et al. proposed this interesting extension of the

classical calculation of fractions. In the concept of fractional derivative with variable order, the order may vary either as a function of the independent differentiation variable (t) or as a function of another (possibly spatial) variable (x), or both. Therefore, the derivative models described using variable-order fractional derivatives are useful and appropriate for the epidemic models. We can obtain the results of fractional order and integer order as a special case from variable-order mathematical models [11–18].

In this article, we will present the theta finite different method with the discretization of new hybrid fractional operator. This operator is called the constant proportional Caputo variable-order fractional derivative (CPC- Θ FDM) and is used to study the proposed model numerically. In the literature, the theta finite differences method (Θ FDM) method, also called the weighted average finite differences method (WAFDM), is one of the finite difference methods [19,20]. This method could be an explicit method or an implicit method (more stable and efficient), depending on the weight factor $\Theta \in [0, 1]$. Using Caputo and Riesz–Feller derivatives, this method was developed for a nonstandard finite difference method [21,22].

The goal of this work is to present and analyze a hybrid variable-order fractional model of multi-vaccination for COVID-19. The new variable-order hybrid derivatives are defined as the linear combination of the variable-order Riemann–Liouville integral and the variable-order derivative of Caputo. This is one of the most effective and reliable of these operators; it is more general than the Caputo fractional operator. Positivity, boundedness and stability will be proved in the current model.

Moreover, one of the aims of this article is developing CPC- Θ FDM for solving the variable-order fractional differential equations numerically and we will compare the obtained results with the results obtained with the fourth order generalized Runge–Kutta method (GRK4M) [23] and the method in [24]. Moreover, we extended the method in [24] to variable order. The analysis of stability and convergence of the proposed method will be studied. Numerical simulations will be given to confirm the efficiency and wide applicability of the proposed method.

To our knowledge, no numerical investigations of a hybrid variable-order fractional for multi-vaccination for a COVID-19 mathematical model utilizing CPC- Θ FDM have been conducted.

This paper is organized as follows: Some notations and definitions of variable-order fractional derivatives are introduced in Section 2. In Section 3, the model with a hybrid variable order is presented; moreover, the positivity, boundedness, existence and uniqueness of the solutions and the stability of the present model are discussed. In Section 4, the numerical methods GRK4M and CPC- Θ SFDM are studied; moreover, stability analyses for these methods are proved. In Section 5, numerical simulations are presented. The conclusions are ultimately outlined in Section 6.

2. Notations and Preliminaries

In this section, we review several key definitions of variable-order calculus that will be utilized throughout the remainder of this article.

Definition 1. Caputo's derivatives (right–left side variable-order fractional $\alpha(t)$) are defined, respectively, as follows [25]:

$$({}^C D_{b-}^{\alpha(t)} f)(x) = ({}^C D_b^{\alpha(t)} f)(t) = \frac{(-1)^n}{\Gamma(n - \alpha(t))} \int_t^b \frac{f^{(n)}(s)}{(s - t)^{-n + \alpha(t) + 1}} ds, \quad b > t, \quad (1)$$

$$({}^C D_{a+}^{\alpha(t)} f)(t) = ({}^C D_t^{\alpha(t)} f)(t) = \frac{1}{\Gamma(n - \alpha(t))} \int_a^t \frac{f^{(n)}(s)}{(t - \xi)^{-n + \alpha(t) + 1}} ds, \quad t > a, \quad (2)$$

$$f(t) \in AC^n[a, b], \quad n = 1 + [\Re(\alpha(t))], \quad \Re(\alpha(t)) \notin \mathbb{N}_0.$$

Definition 2. Let $1 > \alpha(t) > 0$, $-\infty < a < b < +\infty$; the right-left side variable-order fractional Riemann–Liouville’s integral and $f(t) \in AC^n[a, b]$ are given as follows [25]:

$${}_t I_b^{\alpha(t)} f(t) = \left[\int_t^b f(s)(t-s)^{\alpha(t)-1} ds \right] \frac{1}{\Gamma(\alpha(t))}, \quad t < b, \quad (3)$$

$${}_a I_t^{\alpha(t)} f(t) = \left[\int_a^t f(s)(t-s)^{\alpha(t)-1} ds \right] \frac{1}{\Gamma(\alpha(t))}, \quad t > a. \quad (4)$$

$$\alpha(t) \in \mathbb{C}.$$

Definition 3 ([26]). The variable-order fractional Caputo proportional operator (CP) is given as follows:

$$\begin{aligned} {}_0^{\text{CP}} D_t^{\alpha(t)} y(t) &= \int_0^t (\Gamma(1-\alpha(t)))^{-1} (t-s)^{-\alpha(t)} (y'(s)K_0(s, \alpha(t)) + y(s)K_1(s, \alpha(t))) ds, \\ &= \left(\frac{\Gamma(1-\alpha(t))^{-1}}{t^{\alpha(t)}} \right) (y'(t)K_0(t, \alpha(t)) + y(t)K_1(t, \alpha(t))). \end{aligned} \quad (5)$$

$$K_1(\alpha(t), t) = (-\alpha(t) + 1)t^{\alpha(t)}, \quad K_0(\alpha(t), t) = t^{(1-\alpha(t))}\alpha(t), \quad 1 > \alpha(t) > 0.$$

Alternatively, the constant proportional Caputo (CPC) variable-order fractional hybrid operator can be formulated as follows [26]:

$$\begin{aligned} {}_0^{\text{CPC}} D_t^{\alpha(t)} y(t) &= \left(\int_0^t (t-s)^{-\alpha(t)} \frac{1}{\Gamma(1-\alpha(t))} (K_1(\alpha(t))y(s) + y'(s)K_0(\alpha(t))) ds \right) \\ &= K_1(\alpha(t)) {}_0^{\text{RL}} I_t^{1-\alpha(t)} y(t) + K_0(\alpha(t)) {}_0^{\text{C}} D_t^{\alpha(t)} y(t), \end{aligned} \quad (6)$$

$$K_0(\alpha(t)) = Q^{(-\alpha(t)+1)}\alpha(t), \quad K_1(\alpha(t)) = Q^{\alpha(t)}(-\alpha(t) + 1), \text{ where } Q \text{ is a constant.}$$

Definition 4. Moreover, its inverse operator is [26]:

$${}_0^{\text{CPC}} I_t^{\alpha(t)} y(t) = \left(\int_0^t \exp \left[\frac{K_1(\alpha(t))}{K_0(\alpha(t))} (t-s) \right] {}_0^{\text{RL}} D_t^{1-\alpha(t)} y(s) ds \right) \frac{1}{K_0(\alpha(t))}. \quad (7)$$

3. A Hybrid Variable-Order Mathematical Model

A variable-order multiple vaccination model for COVID-19 is presented below; it is an extension of the model given in [24]. To satisfy the dimensional fit between the two sides of the resulting variable-order fraction equations, the variable-order operator is modified by an auxiliary parameter σ . As a result, the dimension of the left side is $(\text{day})^{-1}$ [27]. The following is the updated variable-order nonlinear fractional mathematical model:

$$\begin{aligned} \frac{1}{\sigma^{1-\alpha(t)}} {}_0^{\text{CPC}} D_t^{\alpha(t)} S &= \Lambda - \nu_1 S - \nu_2 S - \nu_3 S - \lambda S - \mu S, \\ \frac{1}{\sigma^{1-\alpha(t)}} {}_0^{\text{CPC}} D_t^{\alpha(t)} V_1 &= \nu_1 S - (1 - \xi_1)\lambda V_1 - \mu V_1, \\ \frac{1}{\sigma^{1-\alpha(t)}} {}_0^{\text{CPC}} D_t^{\alpha(t)} V_2 &= \nu_2 S - (1 - \xi_2)\lambda V_2 - \mu V_2, \\ \frac{1}{\sigma^{1-\alpha(t)}} {}_0^{\text{CPC}} D_t^{\alpha(t)} V_3 &= \nu_3 S - (1 - \xi_3)\lambda V_3 - \mu V_3, \\ \frac{1}{\sigma^{1-\alpha(t)}} {}_0^{\text{CPC}} D_t^{\alpha(t)} A &= f_3(1 - \xi_3)\lambda V_3 + f_2(1 - \xi_2)\lambda V_2 + f_1(1 - \xi_1)\lambda V_1 - (\gamma_A + \mu)A + p\lambda S, \end{aligned}$$

$$\begin{aligned}
\frac{1}{\sigma^{1-\alpha(t)}} {}_0^{\text{CPC}} D_t^{\alpha(t)} I_U &= (1-p)\lambda S - (\gamma_{IU} + d_{IU} + \alpha_1 \mu) I_U, \\
\frac{1}{\sigma^{1-\alpha(t)}} {}_0^{\text{CPC}} D_t^{\alpha(t)} I_V &= (1-f_2)(1-\xi_2)\lambda V_2 + (1-f_3)(1-\xi_3) + (1-f_1)(1-\xi_1)\lambda V_1 \lambda V_3 \\
&\quad - (\gamma_{IV} + (1-\phi)\alpha\mu + d_{IV}) I_V, \\
\frac{1}{\sigma^{1-\alpha(t)}} {}_0^{\text{CPC}} D_t^{\alpha(t)} I_S &= \alpha_1(1-\phi) I_V - (d_{IS} + \mu + \gamma_{IS}) I_S + \alpha_1 I_U, \\
\frac{1}{\sigma^{1-\alpha(t)}} {}_0^{\text{CPC}} D_t^{\alpha(t)} R &= \gamma_A A + \gamma_{IU} I_U + \gamma_{IV} I_V + \gamma_{IS} I_S - \mu R.
\end{aligned} \tag{8}$$

$$\lambda = \beta N_H^{-1} \left(I_U + \theta A + \eta_v I_v \right),$$

$$S + V_1 + V_2 + V_3 + A + I_U + I_V + I_S + R = N_H(t),$$

with the initial conditions

$$\begin{aligned}
S(0) = s_0 \geq 0, \quad V_1(0) = v_{10} \geq 0, \quad V_2 = v_{20} \geq 0, \quad V_3 = v_{30} \geq 0, \quad A = a_0 \geq 0, \quad I_U = i_{u0} \geq 0, \\
I_V = i_{v0} \geq 0, \quad I_S = i_{s0}, \quad R(0) = r_0 \geq 0.
\end{aligned} \tag{9}$$

Figure 1 shows the flowchart of the model (8). Table 1 shows the definitions of variables for system (8). The hypotheses of the model for the rate of each type of vaccination are the same as in [24], as follows:

- 1 $N_H(t) = S + V_1 + V_2 + V_3 + A + I_u + I_v + I_s + R$.
- 2 Vaccination simulations of the proposed model in the strategy implementing only the Pfizer vaccine ($f_1 \neq 0, \xi_1 \neq 0, \phi_1 \neq 0, v_1 \neq 0$), where these parameters are defined as in Table 2.
- 3 Vaccination simulations of the proposed model in the strategy implementing only Moderna vaccine ($\xi_2 \neq 0, f_2 \neq 0, v_2 \neq 0, \phi_2 \neq 0$).
- 4 Vaccination simulations of the proposed model in the strategy implementing only Janssen vaccine ($\xi_3 \neq 0, f_3 \neq 0, v_3 \neq 0, \phi_3 \neq 0$).

We can verify the boundedness of the solution for the suggested model (8) as follows:

$$\begin{aligned}
&\frac{1}{\sigma^{1-\alpha(t)}} ({}_0^{\text{CPC}} D_t^{\alpha(t)} S + {}_0^{\text{CPC}} D_t^{\alpha(t)} R + {}_0^{\text{CPC}} D_t^{\alpha(t)} V_3 + {}_0^{\text{CPC}} D_t^{\alpha(t)} V_2 + {}_1^{\text{CPC}} D_t^{\alpha(t)} V + \\
&{}_0^{\text{CPC}} D_t^{\alpha(t)} A + {}_0^{\text{CPC}} D_t^{\alpha(t)} S + {}_0^{\text{CPC}} D_t^{\alpha(t)} I_S + {}_0^{\text{CPC}} D_t^{\alpha(t)} I_V + {}_0^{\text{CPC}} D_t^{\alpha(t)} I_U) = \sigma^{-1+\alpha(t)} {}_0^{\text{CPC}} D_t^{\alpha(t)} N_H(t), \\
&\frac{1}{\sigma^{1-\alpha(t)}} {}_0^{\text{CPC}} D_t^{\alpha(t)} N_H(t) = \Lambda - \mu N_H(t) - [d_{IV} I_V + d_{IU} I_U + d_{IS} I_S], \quad N_H(0) = A \geq 0,
\end{aligned} \tag{10}$$

$$\Lambda - (\mu + 3\delta) N_H \leq \frac{dN_H}{dt} < \Lambda - \mu N_H, \quad \delta = \min\{d_{IV}, d_{IU}, d_{IS}\}.$$

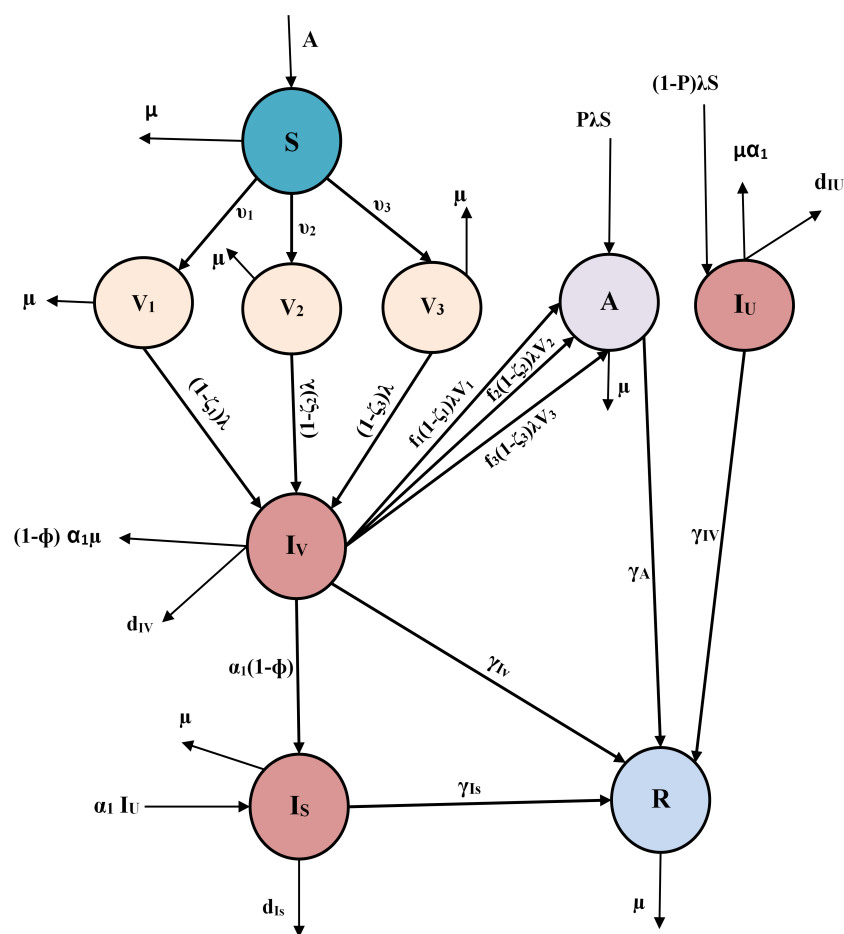
Therefore, we have $N_H(t) \leq \Lambda \mu^{-1}$, at $t \rightarrow \infty$. The feasible region

$$\Omega = \{S, A, I_U, I_V, I_S, R, V_3, V_1, V_2 \in \mathbb{R}^9, N_H(t) \leq \Lambda \mu^{-1}\}.$$

System (8) has a solution in Ω . This verifies the boundedness of the solution.

Table 1. Variables of system (8).

Variable	Interpretation
R	Humans who have recovered
S	Unvaccinated susceptible individuals
V_3	Vaccinated using vaccination number three (Oxford Johnson & Johnson)
V_2	Vaccinated using vaccination number two (Moderna)
V_1	Vaccinated using vaccination number one (Pfizer)
I_S	Individuals with severe sickness and hospitalization who are symptomatic (vaccinated and unvaccinated) (under complete isolation)
I_V	Symptomatic people who have been vaccinated
I_U	Symptomatic people who have not been immunized
A	Asymptomatic individuals (vaccinated and unvaccinated)

**Figure 1.** Flowchart for system (8).

Theorem 1. Using (9), for $t \geq 0$ solutions of (8) are still nonnegative.

Proof. Using (9), we obtain [28]:

$$\begin{aligned}
& \frac{1}{\sigma^{1-\alpha(t)}_0} {}^{CPC}D_t^{\alpha(t)} S|_{S=0} = \Lambda \geq 0, \\
& \frac{1}{\sigma^{1-\alpha(t)}_0} {}^{CPC}D_t^{\alpha(t)} V_1|_{V_1=0} = V_1 S \geq 0, \\
& \frac{1}{\sigma^{1-\alpha(t)}_0} {}^{CPC}D_t^{\alpha(t)} V_2|_{V_2=0} = V_2 S \geq 0, \\
& \frac{1}{\sigma^{1-\alpha(t)}_0} {}^{CPC}D_t^{\alpha(t)} V_3|_{V_3=0} = V_3 S \geq 0, \\
& \frac{1}{\sigma^{1-\alpha(t)}_0} {}^{CPC}D_t^{\alpha(t)} A|_{A=0} = (1 - \xi_2)f_2\lambda V_2 + (1 - \xi_3)f_3\lambda V_3 + p\lambda S + (1 - \xi_1)f_1\lambda V_1 \geq 0, \\
& \frac{1}{\sigma^{1-\alpha(t)}_0} {}^{CPC}D_t^{\alpha(t)} I_U|_{I_U=0} = (1 - p)\lambda S \geq 0, \\
& \frac{1}{\sigma^{1-\alpha(t)}_0} {}^{CPC}D_t^{\alpha(t)} I_V|_{I_V=0} = (1 - \xi_2)\lambda(1 - f_2)V_2 + (1 - \xi_3)\lambda V_3(1 - f_3) + (1 - \xi_1)\lambda V_1(1 - f_1) \geq 0, \\
& \frac{1}{\sigma^{1-\alpha(t)}_0} {}^{CPC}D_t^{\alpha(t)} I_S|_{I_S=0} = \alpha_1 I_U + (1 - \phi)\alpha_1 I_V \geq 0, \\
& \frac{1}{\sigma^{-\alpha(t)+1}_0} {}^{CPC}D_t^{\alpha(t)} R|_{R=0} = \gamma_A A + \gamma_{IU} I_U + \gamma_{IV} I_V + \gamma_{IS} I_S \geq 0.
\end{aligned} \tag{11}$$

□

3.1. Uniqueness and Existence

The existence and uniqueness of the solutions of the proposed model will be established using Banach fixed point theorem. Let system (8) be written as follows [4]:

$${}_0^{CPC}D_t^{\alpha(t)} \varepsilon(t) = \omega(\varepsilon(t), t), \quad \varepsilon(0) = \varepsilon_0 \geq 0, \tag{12}$$

$\varepsilon(t) = \left(S, A, I_U, I_V, I_S, R, V_3, V_1, V_2 \right)^T$ represents the variables of the proposed system (8) and ω is a vector that represents the equations in the right of the system (8).

$$\begin{pmatrix} \omega_1 \\ \omega_2 \\ \omega_3 \\ \omega_4 \\ \omega_5 \\ \omega_6 \\ \omega_7 \\ \omega_8 \\ \omega_9 \end{pmatrix} = \begin{pmatrix} \sigma^{1-\alpha(t)} (\Lambda - v_1 S - v_2 S - v_3 S - \lambda S - \mu S) \\ \sigma^{1-\alpha(t)} (v_1 S - (1 - \xi_1)\lambda V_1 - \mu V_1) \\ \sigma^{1-\alpha(t)} (v_1 S - (1 - \xi_2)\lambda V_2 - \mu V_2) \\ \sigma^{1-\alpha(t)} (v_1 S - (1 - \xi_3)\lambda V_3 - \mu V_3) \\ \sigma^{1-\alpha(t)} ((1 - \xi_2)\lambda f_2 V_2 + (1 - \xi_1)\lambda f_1 V_1 + (1 - \xi_3)\lambda f_3 V_3 - (\gamma_A + \mu)A) + p\lambda S \\ \sigma^{1-\alpha(t)} ((1 - p)\lambda S - (\gamma_{IU} + d_{IU} + \alpha_1 \mu)I_U) \\ \sigma^{1-\alpha(t)} ((1 - \xi_2)\lambda(1 - f_2)V_2 + (1 - \xi_3)\lambda(1 - f_3)V_3 + (1 - \xi_1)\lambda(1 - f_1)V_1 - (d_{IV} + \alpha(1 - \phi)\mu)I_V + \gamma_{IV}) \\ \sigma^{1-\alpha(t)} (\alpha_1 I_U - (d_{IS} + \mu + \gamma_{IS})I_S) + \alpha_1(1 - \phi)I_V \\ \sigma^{1-\alpha(t)} (\gamma_{IU} I_U + \gamma_{IV} I_V + \gamma_{IS} I_S - \mu R + \gamma_A A) \end{pmatrix},$$

with an initial condition ε_0 . Furthermore, Lipschitz requirements as in [4] are satisfied:

$$\|\omega(\varepsilon_1(t), t) - \omega(\varepsilon_2(t), t)\| \leq W^0 \|\varepsilon_1(t) - \varepsilon_2(t)\|, \quad W^0 \in \mathbb{R}. \tag{13}$$

Theorem 2. *If the following conditions are met:*

$$\frac{W^0 F_{\max}^{\alpha(t)} X_{\max}^{\alpha(t)}}{\Gamma(\alpha(t) - 1) K_0(\alpha(t))} < 1, \tag{14}$$

the hybrid variable-order fractional model (8) has a unique solution.

Proof. Applying (6) in (12), we have:

$$\varepsilon(t) = \varepsilon(t_0) + \frac{1}{K_0(\alpha(t))} \int_0^t \exp\left(-\frac{K_1(\alpha(t))}{K_0(\alpha(t))}(t-s)\right) {}_0^{RL}D_t^{1-\alpha(t)} \omega(\varepsilon(s), s) ds. \tag{15}$$

Let $B : C(K, \mathbb{R}^9) \rightarrow C(K, \mathbb{R}^9)$ and $K = (0, T)$; then:

$$B[\varepsilon(t)] = \varepsilon(t_0) + \frac{1}{K_0(\alpha(t))} \int_0^t \exp\left(-\frac{K_1(\alpha(t))}{K_0(\alpha(t))}(t-s)\right) {}_0^{RL}D_t^{1-\alpha(t)} \omega(\varepsilon(s), s) ds. \quad (16)$$

We have:

$$B[\varepsilon(t)] = \varepsilon(t).$$

The supremum norm on K is represented by $\|\cdot\|_K$. Thus

$$\|\varepsilon(t)\|_K = \sup_{t \in K} \|\varepsilon(t)\|, \quad \varepsilon(t) \in C(K, \mathbb{R}^9).$$

So, $\|\cdot\|_K$ with $C(K, \mathbb{R}^9)$ is a Banach space. Then, the following relation holds:

$$\Lambda \|\varphi(s, t)\|_K \|\varepsilon(s)\|_K \geq \left\| \int_0^t \varphi(s, t) \varepsilon(s) ds \right\|, \quad 0 < t < \Lambda < \infty$$

with $\varphi(s, t) \in C(K^2, \mathbb{R}^9)$ $\varepsilon(t) \in C(K, \mathbb{R}^9)$,

then $\sup_{t, s \in K} |\varphi(s, t)| = \|\varphi(s, t)\|_K$.

Relation (16) can be written as:

$$\begin{aligned} \|B[\varepsilon_1(t)] - B[\varepsilon_2(t)]\|_K &\leq \left\| \frac{1}{K_0(\alpha(t))} \int_0^t \exp\left(-\frac{K_1(\alpha(t))}{K_0(\alpha(t))}(t-s)\right) {}_0^{RL}D_t^{1-\alpha(t)} \omega(\varepsilon_1(s), s) \right. \\ &\quad \left. - {}_0^{RL}D_t^{1-\alpha(t)} \omega(\varepsilon_2(s), s) ds \right\|_K \\ &\leq \frac{F_{\max}^{\alpha(t)}}{K_0(\alpha(t))\Gamma(\alpha(t)-1)} \left\| \int_0^t (t-s)^{\alpha(t)-2} (\omega(\varepsilon_1(s), s) - \omega(\varepsilon_2(s), s)) ds \right\|_K \\ &\leq \frac{F_{\max}^{\alpha(t)} X_{\max}^{\alpha(t)}}{K_0(\alpha(t))\Gamma(\alpha(t)-1)} \|\omega(\varepsilon_1(t), t) - \omega(\varepsilon_2(t), t)\|_K \\ &\leq \frac{W^0 F_{\max}^{\alpha(t)} X_{\max}^{\alpha(t)}}{K_0(\alpha(t))\Gamma(\alpha(t)-1)} \|\varepsilon_1(t) - \varepsilon_2(t)\|_K. \end{aligned} \quad (17)$$

Then

$$\|B[\varepsilon_1(t)] - B[\varepsilon_2(t)]\|_K \leq L \|\varepsilon_1(t) - \varepsilon_2(t)\|_K, \quad (18)$$

where

$$L = \frac{W^0 F_{\max}^{\alpha(t)} X_{\max}^{\alpha(t)}}{K_0(\alpha(t))\Gamma(\alpha(t)-1)}.$$

B is a contraction operator if $1 > L$. So (8) has a unique solution. \square

Table 2. The definition of all parameters of system (8).

Parameter	Interpretation	Baseline Value (per day ⁻¹)	Reference
Λ	Recruitment rate	$\frac{29,200,000}{75 \times 365} \text{ day}^{-1}$	[29]
β	Rate of effective transmission	0.00016708	[24]
μ	Natural death rate	$\frac{1}{75 \times 365} \text{ day}^{-1}$	[29]
ξ_3	Efficacy of the Janssen vaccine	0.67	[1]
ξ_2	Efficacy of the Moderna vaccine	0.945	[30]
ξ_1	Efficacy of the Pfizer vaccine	0.95	[31]
ν_3	Rate of Janssen vaccination	0.00053 day^{-1}	[24]
ν_2	Rate of Moderna vaccination	0.0042 day^{-1}	[24]
ν_1	Rate of Pfizer vaccination	0.0059 day^{-1}	[24]
p	Unvaccinated susceptibles who move to the asymptomatic stage are a small percentage of the total	0.5	[24]
θ	A parameter was changed to limit the transmissibility of asymptomatic people	0.7	[32]
ϕ	Vaccine effectiveness against severe COVID-19 sickness	0.8	[2]
f_i	The percentage of susceptibles who received the vaccine and went on to develop subclinical disease	0.5	[24]
$\gamma_A, \gamma_{IU}, \gamma_{IV}, \gamma_{IS}$	Individuals in A, I_U, I_V and I_S classes, respectively; the programme has a high rate of recovery	0.13978 day^{-1}	[24]
d_{IU}, d_{IV}, d_{IS}	Death rates from disease for people in the I_U, I_V and I_S groups, respectively	0.015	[32]
α_1	The rate at which severe COVID-19 sickness develops	0.3	[32]

3.2. Local Stability

The basic reproduction number is calculated in this section. The next generation operator method is used to investigate the local stability of the disease-free equilibrium (DFE), which is given by solving $\frac{1}{\sigma^{1-\alpha(t)}} {}^{CPC}D_t^{\alpha(t)}(.) = 0$ of model (8) and considering $I_U = I_V = I_S = 0$. Then, we obtained D_0 , where D_0 is the DFE and is given by [33]:

$$D_0 = (\tilde{S}, \tilde{V}_3, \tilde{V}_2, \tilde{V}_1, \tilde{A}, \tilde{I}_V, \tilde{I}_S, \tilde{I}_U, \tilde{R}) = \left(\frac{\Lambda}{(\nu_3 + \nu_2 + \nu_1 + \mu)}, \frac{\nu_3 \Lambda}{(\nu_3 + \nu_2 + \nu_1 + \mu)}, \frac{\nu_2 \Lambda}{(\nu_3 + \nu_2 + \nu_1 + \mu)}, \frac{\nu_1 \Lambda}{(\nu_1 + \nu_2 + \nu_3 + \mu)}, \frac{\Lambda}{(\nu_1 + \nu_2 + \nu_3 + \mu)}, 0, 0, 0, 0 \right).$$

As a result, the matrix V of the transfer of individuals between compartments and the matrix F of new infection terms are provided by

$$F = \sigma^{1-\alpha(t)} \begin{pmatrix} \frac{\beta \theta \tilde{Q}}{\tilde{N}_H} & \frac{\beta \tilde{Q}}{\tilde{N}_H} & \frac{\beta \eta_V \tilde{Q}}{\tilde{N}_H} & 0 \\ (1-p) \frac{\beta \theta \tilde{S}}{\tilde{N}_H} & (1-p) \frac{\beta \tilde{S}}{\tilde{N}_H} & (1-p) \frac{\beta \eta_V \tilde{S}}{\tilde{N}_H} & 0 \\ \frac{\beta \theta \tilde{v}}{\tilde{N}_H} & \frac{\beta \tilde{v}}{\tilde{N}_H} & \frac{\beta \eta_V \tilde{v}}{\tilde{N}_H} & 0 \\ 0 & 0 & 0 & 0 \end{pmatrix},$$

with $\tilde{v} = (1 - \xi_3)(1 - f_3)\tilde{V}_3 + (1 - \xi_2)(1 - f_2)\tilde{V}_2 + (1 - \xi_1)(1 - f_1)\tilde{V}_1$,
 $\tilde{Q} = (1 - \xi_3)f_3\tilde{V}_3 + (1 - \xi_1)f_1\tilde{V}_1 + (1 - \xi_2)f_2\tilde{V}_2 + p\tilde{S}$.

$$V = \sigma^{1-\alpha(t)} \begin{pmatrix} \mu + \gamma_A & 0 & 0 & 0 \\ 0 & \gamma_{IU} + d_{IU} + \alpha_1 + \mu & 0 & 0 \\ 0 & 0 & \gamma_{IV} + d_{IV} + (1 - \phi)\alpha_1 + \mu & 0 \\ 0 & -\alpha_1 & -(1 - \phi)\alpha_1 & \gamma_{IU} + d_{IU} + \mu \end{pmatrix}.$$

The model's basic reproduction number, denoted by R_0 , is given by [34,35]:

$$\rho(FV^{-1}) = R_0 = \sigma^{1-\alpha(t)} \beta \left(\frac{(1-p)E_1E_3\mu + E_1E_2\eta_VY_1 + E_2E_3\eta_A\theta Y_2}{\mu(\nu_1 + \nu_2 + \nu_3)E_1E_2E_3} \right). \quad (19)$$

with $E_1 = (\gamma_A + \mu)$,

$E_2 = (\gamma_{IU} + d_{IU} + \alpha_1 + \mu)$,

$E_3 = (\alpha_1(1 - \phi) + d_{IV} + \mu + \gamma_{IV})$,

$Y_1 = (1 - \xi_3)(1 - f_3)\nu_3 + (1 - \xi_1)(1 - f_1)\nu_1 + (1 - \xi_2)(1 - f_2)\nu_2$,

$Y_2 = (1 - \xi_3)f_3\nu_3 + (1 - \xi_2)f_2\nu_2 + \mu p(1 - \xi_1)f_1\nu_1$.

Theorem 3. The disease-free equilibrium point D_0 of model (8) is locally asymptotically stable (LAS) if $R_0 < 1$ and unstable if $R_0 > 1$.

Proof. The Jacobian matrix of the system (8) at the DFE is used to investigate the local stability of model (8) [33,36].

$$J(D_0) = \sigma^{1-\alpha(t)} \begin{pmatrix} X & 0 & 0 & 0 & A_1 & A_2 & A_3 & 0 & 0 \\ \nu_1 & -\mu & 0 & 0 & B_1 & B_2 & B_3 & 0 & 0 \\ \nu_2 & 0 & -\mu & 0 & F_1 & F_2 & F_3 & 0 & 0 \\ \nu_3 & 0 & 0 & -\mu & G_1 & G_2 & G_3 & 0 & 0 \\ 0 & 0 & 0 & 0 & M_1 & M_2 & M_3 & 0 & 0 \\ 0 & 0 & 0 & 0 & N_1 & N_2 & N_3 & 0 & 0 \\ 0 & 0 & 0 & 0 & Z_1 & Z_2 & Z_3 & 0 & 0 \\ 0 & 0 & 0 & 0 & 0 & \alpha_1 & (1 - \phi)\alpha_1 & -E_4 & 0 \\ 0 & 0 & 0 & 0 & \gamma_A & \gamma_{IU} & \gamma_{IV} & \gamma_{IS} & -\mu \end{pmatrix},$$

where $X = -(\nu_1 + \nu_2 + \nu_3 + \mu)$, $A_1 = -\frac{\beta\theta\tilde{S}_H}{N_H}$, $A_2 = -\frac{\beta\tilde{S}_H}{N_H}$, $A_3 = -\frac{\beta\eta_V\tilde{S}_H}{N_H}$,
 $B_1 = -(1 - \zeta_1)\frac{\beta\theta\tilde{V}_1}{N_H}$, $B_2 = -(1 - \zeta_1)\frac{\beta\tilde{V}_1}{N_H}$, $B_3 = -(1 - \zeta_1)\frac{\beta\eta_V\tilde{V}_1}{N_H}$,
 $F_1 = -(1 - \zeta_2)\frac{\beta\theta\tilde{V}_2}{N_H}$, $F_2 = -(1 - \zeta_2)\frac{\beta\tilde{V}_2}{N_H}$, $F_3 = -(1 - \zeta_2)\frac{\beta\eta_V\tilde{V}_2}{N_H}$,
 $G_1 = -(1 - \zeta_3)\frac{\beta\theta\tilde{V}_3}{N_H}$, $G_2 = -(1 - \zeta_3)\frac{\beta\tilde{V}_3}{N_H}$, $G_3 = -(1 - \zeta_3)\frac{\beta\eta_V\tilde{V}_3}{N_H}$,
 $M_1 = \frac{\beta\theta\tilde{Q}}{N_H} - E_1$, $M_2 = \frac{\beta\tilde{Q}}{N_H}$, $M_3 = \frac{\beta\eta_V\tilde{Q}}{N_H}$,
 $N_1 = \frac{\beta\theta(1-p)\tilde{S}_H}{N_H}$, $N_2 = \frac{\beta(1-p)\tilde{S}_H}{N_H} - E_2$, $N_3 = \frac{\beta(1-p)\eta_V\tilde{S}_H}{N_H}$,
 $Z_1 = \frac{\beta\theta\tilde{v}}{N_H}$, $Z_2 = \frac{\beta\tilde{v}}{N_H}$, $Z_3 = \frac{\beta\eta_V\tilde{v}}{N_H} - E_3$,
 $E_4 = (\gamma_{IS} + d_{IS} + \mu)$.

The characteristic equation:

$$(\nu_3 + \nu_1 + \nu_2 + \mu + \lambda)(\lambda^3 + (E_1 + E_2 + E_3 - \frac{(1-p)\tilde{S} + \eta_V\tilde{v} + \eta_V\theta\tilde{Q}}{N_H})\beta)\lambda^2 + (E_1E_2 + E_1E_3 + E_2E_3 - \beta[(E_1 + E_3)(1-p)\tilde{S} + (E_1 + E_2)\eta_V\tilde{v} + (E_2 + E_3)\eta_A\theta\tilde{Q}])\lambda + E_1E_2E_3(1 - R_0))(\mu + \lambda)^4(\lambda + E_4) = 0.$$

Then, we have

$$(\lambda + \mu) = 0, (\lambda + E_4) = 0, (\lambda + \nu_1 + \nu_2 + \nu_3 + \mu) = 0;$$

the arguments are $\arg(\lambda_k) > \frac{\pi}{a} > k\frac{2\pi}{a} > \frac{\pi}{M} > \frac{\pi}{2M}$, where $k = 0, 1, 2, 3, \dots, a - 1$.

$$(\lambda^3 + (E_1 + E_2 + E_3 - \beta\frac{(1-p)\tilde{S} + \eta_V\tilde{v} + \eta_V\theta\tilde{Q}}{N_H})\lambda^2 + (E_1E_2 + E_1E_3 + E_2E_3 - \beta[(E_1 + E_3)(1-p)\tilde{S} + (E_1 + E_2)\eta_V\tilde{v} + (E_2 + E_3)\eta_A\theta\tilde{Q}])\lambda + E_1E_2E_3(1 - R_0)) = 0.$$

We can rewrite the above equation as:

$$\lambda^3 + a\lambda^2 + b\lambda + c = 0, \quad (20)$$

where

$$a = (E_1 + E_2 + E_3 - \beta\frac{(1-p)\tilde{S} + \eta_V\tilde{v} + \eta_V\theta\tilde{Q}}{N_H}),$$

$$b = (E_1E_2 + E_1E_3 + E_2E_3 - \beta[(E_1 + E_3)(1-p)\tilde{S} + (E_1 + E_2)\eta_V\tilde{v} + (E_2 + E_3)\eta_A\theta\tilde{Q}]),$$

$$c = E_1E_2E_3(1 - R_0).$$

$$\lambda^3 + a\lambda^2 + b\lambda + c = 0, \quad (21)$$

We obtain

$$\lambda^3 + a\lambda^2 + b\lambda + c = (\lambda - \zeta_{11})(\lambda^2 - \tau\lambda + \zeta_{11}), \quad (22)$$

$$\tau = -(a + \zeta_{11}), \quad (23)$$

$$\zeta_{11} = b + \zeta_{11}(a + \zeta_{11}), \quad (24)$$

$$c = -\zeta_{11}\delta_{11}, \quad (25)$$

Hence, the other two roots are given by

$$\zeta_{11,2,3} = \frac{1}{2}(\tau \pm \sqrt{\Delta}), \quad (26)$$

$$\Delta = \tau^2 - 4\delta_{11} = a^2 - 2a\zeta_{11} - (3\zeta_{11}^2 + 4b). \quad (27)$$

These two roots are complex conjugate when $\Delta < 0$, real and distinct when $\Delta > 0$, and real and coincident when $\Delta = 0$.

Considering that $\Delta = 0$ occurs $a = \zeta_{11} \pm 2\sqrt{\zeta_{11}^2 + b}$, we have that if $\zeta_{11}^2 + b < 0$, then $\Delta > 0$ and two distinct real roots given by

$$\zeta_{11,2,3} = \frac{1}{2}(\tau \pm \sqrt{\Delta}).$$

If $\zeta_{11}^2 + b = 0$ then $\Delta = (a - \zeta_{11})^2$ and two distinct real roots exist given by

$$\zeta_{11,2,3} = \frac{1}{2}(\tau \pm |a - \zeta_{11}|).$$

So that $\zeta_{11,2} = -\zeta_{11,1}$ and $\zeta_{11,3} = -a$, if $\zeta_{11,1}^2 + b > 0$ and $(\zeta_{11} - 2\sqrt{\zeta_{11}^2 + b}) < a < (\zeta_{11} + 2\sqrt{\zeta_{11}^2 + b})$, then $\Delta < 0$ and two complex conjugate roots exist, given by $\zeta_{11,2,3} = \alpha_{11} \pm iB_{11}$ where $\alpha_{22} = \frac{\tau}{2}$, $B_{11} = \frac{\sqrt{4\delta_{11} - \tau_2}}{2} = \sqrt{\delta_{11} - a_{11}^2}$. $a = (\zeta_{11} - 2\sqrt{(\zeta_{11}^2) + b})$ or $a = (\zeta_{11} - 2\sqrt{(\zeta_{11}^2) + a_2})$, then $(\Delta = 0)$ and two coincident real roots exist given by $\zeta_{11,2} = \zeta_{11,3} = \frac{\tau}{2} = \frac{a + \zeta_{11}}{2}$ $a < (\zeta_{11} - 2\sqrt{(\zeta_{11}^2) + a_2})$ or $a_1 > (\zeta_{11} - 2\sqrt{(\zeta_{11}^2) + b})$. Then, $\Delta = 0$ and two distinct real roots exist given by

$$\zeta_{11,2,3} = \frac{1}{2}(\tau \pm \sqrt{\Delta}).$$

Applying the Routh–Hurwitz criterion [37], Equation (27) has roots with negative real parts if and only if $R_0 < 1$. Thus, the DFE is locally asymptotically stable. \square

4. Numerical Methods for Solving the Proposed Model

4.1. GRK4M

Consider the fractional derivatives with variable order given by the following equation:

$${}_0^C D_t^{\alpha(t)} \varepsilon(t) = f(t, \varepsilon(t)), \quad T_f \geq t > 0, \quad 1 \geq \alpha(t) > 0, \quad (28)$$

$$\varepsilon(0) = \varepsilon_0.$$

Using GRK4M [23], the approximate solution of (28) is:

$$\varepsilon_{n+1} = \varepsilon_n + \frac{1}{6}(K_1 + 2K_2 + 2K_3 + K_4), \quad (29)$$

$$K_1 = Yf(t_n, \varepsilon_n),$$

$$K_2 = Yf(t_n + \frac{1}{2}Y, \varepsilon_n + \frac{1}{2}K_1),$$

$$K_3 = Yf(t_n + \frac{1}{2}Y, \varepsilon_n + \frac{1}{2}K_2),$$

$$K_4 = Yf(t_n + Y, \varepsilon_n + K_3),$$

$$\text{where } Y = \frac{\tau^{\alpha(t_n)}}{\Gamma(\alpha(t_n) + 1)}.$$

4.2. Stability of GRK4M

To investigate the stability of GRK4M, we shall utilize the following test problem of variable-order linear differential equation for simplicity:

$${}_0^C D_t^{\alpha(t)} \varepsilon(t) = \varepsilon(t)v, \quad T_f \geq t > 0, \quad v < 0, \quad 1 \geq \alpha(t) > 0, \quad (30)$$

$$\varepsilon(0) = \varepsilon_0.$$

As in [23], Equation (30) is written as follows:

$$\varepsilon(t_{i+1}) = \varepsilon(t_i) + \frac{1}{6} \frac{v \tau^{\alpha(t_i)}}{\Gamma(1 + \alpha(t_i))} \varepsilon(t_i), \quad i = 0, 1, \dots, n-1. \quad (31)$$

Then, we have the following equation [38]:

$$\varepsilon(t_{i+1}) = \left(1 + \frac{1}{6} \frac{\tau^{\alpha(t_i)} v}{\Gamma(1 + \alpha(t_i))}\right)^i \varepsilon_0. \quad (32)$$

The condition of stability [38]:

$$-1 < \left(\frac{1}{6} \frac{\tau^{\alpha(t_i)} v}{\Gamma(1 + \alpha(t_i))} + 1\right) < 1.$$

4.3. CPC- Θ FDM

Consider:

$${}_0^{CPC} D_t^{\alpha(t)} \varepsilon(t) = \zeta(t, \varepsilon(t)), \quad \varepsilon(0) = \varepsilon_0, \quad 1 \geq \alpha(t) > 0. \quad (33)$$

Relationship (6) can be expressed as follows:

$$\begin{aligned} {}_0^{CPC} D_t^{\alpha(t)} \varepsilon(t) &= \frac{1}{\Gamma(1 - \alpha(t))} \int_0^t (t-s)^{-\alpha(t)} (K_1(\alpha(t)) \varepsilon(s) + K_0(\alpha(t)) \varepsilon'(s)) ds, \\ &= K_1(\alpha)_0^{RL} I_t^{1-\alpha(t)} \varepsilon(t) + K_0(\alpha(t)) {}_0^C D_t^{\alpha(t)} \varepsilon(t), \\ &= K_1(\alpha)_0^{RL} D_t^{\alpha(t)-1} \varepsilon(t) + K_0(\alpha(t)) {}_0^C D_t^{\alpha(t)} \varepsilon(t), \end{aligned} \quad (34)$$

Using Θ FDM and GL-approximation, we can discretize (34) as shown below:

$$\begin{aligned} {}_0^{CPC} D_t^{\alpha(t)} \varepsilon(t)|_{t=t^n} &= \frac{K_1(\alpha(t_n))}{\tau^{\alpha(t_n)-1}} \left(\varepsilon_{n+1} + \sum_{i=1}^{n+1} \omega_i \varepsilon_{n+1-i} \right) \\ &\quad + \frac{K_0(\alpha(t_n))}{\tau^{\alpha_n}} \left(\varepsilon_{n+1} - \sum_{i=1}^{n+1} \varrho_i \varepsilon_{n+1-i} - \varsigma_{n+1} \varepsilon_0 \right), \end{aligned} \quad (35)$$

$$\begin{aligned} &\frac{K_1(\alpha(t_n))}{\tau^{\alpha(t_n)-1}} \left(\varepsilon_{n+1} + \sum_{i=1}^{n+1} \omega_i \varepsilon_{n+1-i} \right) + \frac{K_0(\alpha(t_n))}{\tau^{\alpha(t_n)}} \left(\varepsilon_{n+1} - \sum_{i=1}^{n+1} \varrho_i \varepsilon_{n+1-i} - \varsigma_{n+1} \varepsilon_0 \right) \\ &= (\Theta) \zeta(\varepsilon(t_n), t_n) + (1 - \Theta) \zeta(\varepsilon(t_{n+1}), t_{n+1}), \end{aligned} \quad (36)$$

where, $\omega_0 = 1$, $\omega_i = (1 - \frac{\alpha(t_n)}{i}) \omega_{i-1}$, $t^n = n\tau$, $\tau = \frac{T_f}{N}$, N is a natural number, $\varrho_i = (-1)^{i-1} \binom{\alpha(t_n)}{i}$, $\varrho_1 = \alpha(t_n)$, $\varsigma_i = \frac{i^{\alpha(t_n)}}{\Gamma(1-\alpha(t_n))}$. Moreover, consider that [39]:

$$0 < \varrho_{i+1} < \varrho_i < \dots < \varrho_1 = \alpha(t_n) < 1,$$

$$0 < \varsigma_{i+1} < \varsigma_i < \dots < \varsigma_1 = \frac{1}{\Gamma(-\alpha(t_n) + 1)}, \quad i = 1, 2, \dots, n+1.$$

Remark 1. If $K_1(\alpha(t)) = 0$ and $K_0(\alpha(t)) = 1$ in (36), we can obtain the discretization of Caputo operator with theta finite difference technique (C- Θ FDM).

4.4. CPC- Θ FDM Stability Analysis

The stability of method (36) will be considered here. We shall utilize the test problem of variable-order linear differential equation, for simplicity:

$$({}_0^{CPC} D_t^{\alpha(t)}) \varepsilon(t) = A \varepsilon(t), \quad t > 0, \quad A < 0, \quad 0 < \alpha(t) \leq 1. \quad (37)$$

By (34) and GL-approximation, we can discretize (37) as shown below:

$$\begin{aligned} & \frac{K_1(\alpha(t_n))}{\tau^{\alpha(t_n)-1}} \left(\varepsilon_{n+1} + \sum_{i=1}^{n+1} \omega_i \varepsilon_{n+1-i} \right) + \frac{K_0(\alpha(t_n))}{\tau^{\alpha(t_n)}} \left(\varepsilon_{n+1} - \sum_{i=1}^{n+1} \varrho_i \varepsilon_{n+1-i} - \varsigma_{n+1} \varepsilon_0 \right) \\ & = \Theta A \varepsilon_n + (1 - \Theta) A \varepsilon_{n+1}; \end{aligned} \quad (38)$$

put $C = \frac{K_1(\alpha(t_n))}{\tau^{\alpha(t_n)-1}}$, $B = \frac{K_0(\alpha(t_n))}{\tau^{\alpha(t_n)}}$. Then, from boundness theorem [40], we have:

$$\varepsilon_{n+1} = \frac{1}{C+B} \left(A \varepsilon_n - C \sum_{i=1}^{n+1} \omega_i \varepsilon_{n+1-i} + B \left(\sum_{i=1}^{n+1} \varrho_i \varepsilon_{n+1-i} + \varsigma_{n+1} \varepsilon_0 \right) \right) \leq \varepsilon_n, \quad (39)$$

This means $\varepsilon_0 \geq \varepsilon_1 \geq \dots \geq \varepsilon_{n-1} \geq \varepsilon_n \geq \varepsilon_{n+1}$. Then, method (36) is stable.

4.5. Convergence of the Method

Equation (34) can be discretized as shown below:

$$\begin{aligned} {}_0^{\text{CPC}} D_t^{\alpha(t)} \varepsilon(t)|_{t=t^n} &= \frac{K_1(\alpha(t_n))}{\tau^{\alpha(t_n)-1}} \left(\varepsilon_{n+1} + \sum_{i=1}^{n+1} \omega_i \varepsilon_{n+1-i} \right) \\ &+ \frac{K_0(\alpha(t_n))}{\tau^{\alpha(t_n)}} \left(\varepsilon_{n+1} - \sum_{i=1}^{n+1} \varrho_i \varepsilon_{n+1-i} - \varsigma_{n+1} \varepsilon_0 \right), \end{aligned} \quad (40)$$

$$\begin{aligned} & \frac{K_1(\alpha(t_n))}{\tau^{\alpha(t_n)-1}} \left(\varepsilon_{n+1} + \sum_{i=1}^{n+1} \omega_i \varepsilon_{n+1-i} \right) + \frac{K_0(\alpha(t_n))}{\tau^{\alpha(t_n)}} \left(\varepsilon_{n+1} - \sum_{i=1}^{n+1} \varrho_i \varepsilon_{n+1-i} - \varsigma_{n+1} \varepsilon_0 \right) \\ & - \Theta \zeta(\varepsilon(t_n), t_n) - (1 - \Theta) \zeta(\varepsilon(t_{n+1}), t_{n+1}) = T_{Rn}, \end{aligned} \quad (41)$$

where

$$\|T_{Rn}\|_{\infty} < W, \quad W = C \max_{0 \leq i \leq n+1} |\varepsilon_{i+1}|,$$

$$C = (\tau^{\alpha(t_i)-1} + \tau^{\alpha(t_i)}).$$

The proposed method is convergent because it is stable and consistent [41], then (41) is convergent.

5. Numerical Results

In the following, we solved (8) numerically using GRK4M (29) and CPC- Θ FDM (36). Using CPC- Θ FDM for solving (8), we obtained $(9N + 9)$ of the nonlinear algebraic system with $(9N + 9)$ unknown.

$$\left(S, V_1, V_2, V_3, A, I_U, I_V, I_S, R \right)$$

can be solved using an appropriate iterative method based on the assumed beginning conditions. For the real data, we use [24]; the authors in this reference used the literature to obtain some parameter values and the remaining values were fitted to the data for the state of Texas, USA. They fitted the data of (8) solutions with the data for the state of Texas from 13 March to 29 June 2021 [29,42]. The model was fitted with three datasets, Moderna, Janssen, and Pfizer, with immunization data for Texas state. The three vaccination rates v_1, v_2 and v_3 corresponding to each vaccine as well as the effective contact rate for COVID-19 transmission, β , are estimated. According to publicly available data, the total population of the state of Texas, USA, for the year 2021 was 29,200,000 [1]. Let $R(0) = 5000$, $V_2(0) = 4,016,005$, $A(0) = 50,000$, $V_3(0) = 129,859$, $S(0) = 24,000,000$, $I_U(0) = 17,000$, $I_V(0) = 15,000$, $V_1(0) = 4,115,127$ and $I_S(0) = 10,000$. The parameter values are given in Table 2. To show that the proposed scheme is efficient, we compare the results that we obtained in this paper with the results that were found in reference [24], which are given in Figure 2 in constant fractional order. Figure 3 shows the behavior of the approximate

solution of (8) (using the method in [24]) with different values of $\alpha(t)$. As can be seen from this figure, when the value of the fractional derivative changes over time, the results are different and this can dramatically affect the behavior of the model. This confirms the generality of the variable-order derivatives. Unfortunately, this method gives us unstable solutions, as in Figure 4a, when the value of the step size equals one. Moreover, we obtained the stable solutions using the proposed method CPC- Θ FDM and $\Theta = 0$, in the fully implicit case given in this paper. This confirms that the method in [24] is stable only when the step size is very small, while our used method is stable regardless of the value of the step size. Figure 5 shows the behavior of the approximate solution of (8) (using CPC- Θ FDM and $\Theta = 0.5, Q = 0.00025$) with different values of $\alpha(t)$. The approximate solution behavior of (8) is shown in Figure 6 ($\Theta = 1$ and using CPC- Θ FDM) with different values of $\alpha(t)$, $Q = 0.00025$. The approximate solution behavior of (8) (using GRK4M with different values of $\alpha(t)$) is shown in Figure 7. Figure 8 shows the behavior of the approximate solution of (8) (using CPC- Θ FDM when $K_0(\alpha(t)) = 1$, $K_1(\alpha(t)) = 0$ and $\Theta = 0$) with different values of $\alpha(t)$. We noted that by comparing our results with different variable orders and constant orders as given in [24] and Figure 5, the result in the case of constant order is agreement. Moreover, by compering the results given in Figures 7 and 8, the result given using CPC- Θ FDM (fully implicit case) is convergent, better than the results given using GRK4 when we use nonlinear $\alpha(t)$. Figure 9 shows the relation between R and I_v, I_u, I_s, A using CPC- Θ FDM (fully implicit case) and nonlinear $\alpha(t)$. Furthermore, we found that the variable-order derivative order model is a more general model than the fractional order model given in [24] and integer order; a new behavior of the solution appears by using different values of $\alpha(t)$. Moreover, we can obtain the fractional Caputo operator as a special case from the CPC operator when $K_0(\alpha(t)) = 1$, $K_1(\alpha(t)) = 0$. Moreover, we can obtain the fractional Caputo operator as a special case from the CPC operator if $K_0(\alpha(t)) = 1$, $K_1(\alpha(t)) = 0$. The solutions obtained using the new method CPC- Θ FDM can be explicit ($\Theta = 1$) or implicit ($0 \leq \Theta \leq 1$), and fully implicit with accurate solution when ($\Theta = 0$).

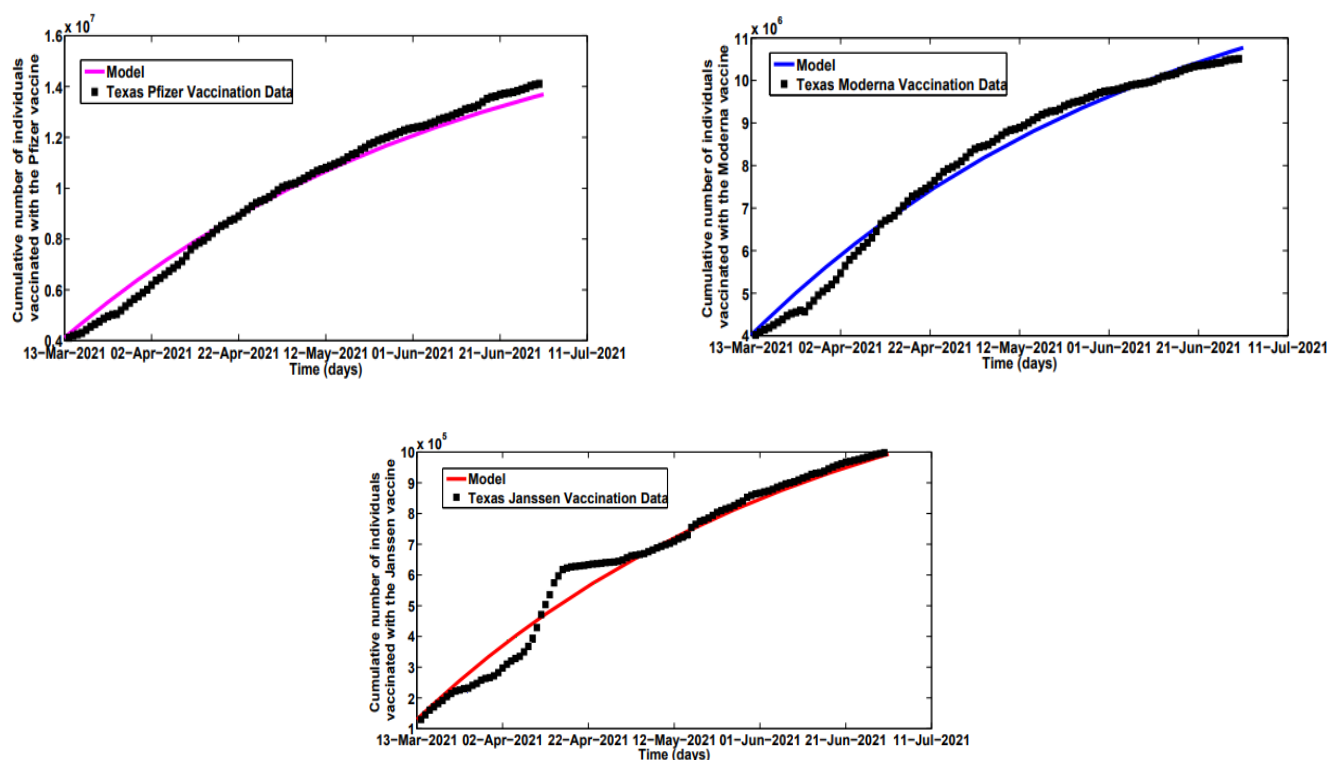


Figure 2. Real data [24] versus fitting model (8).

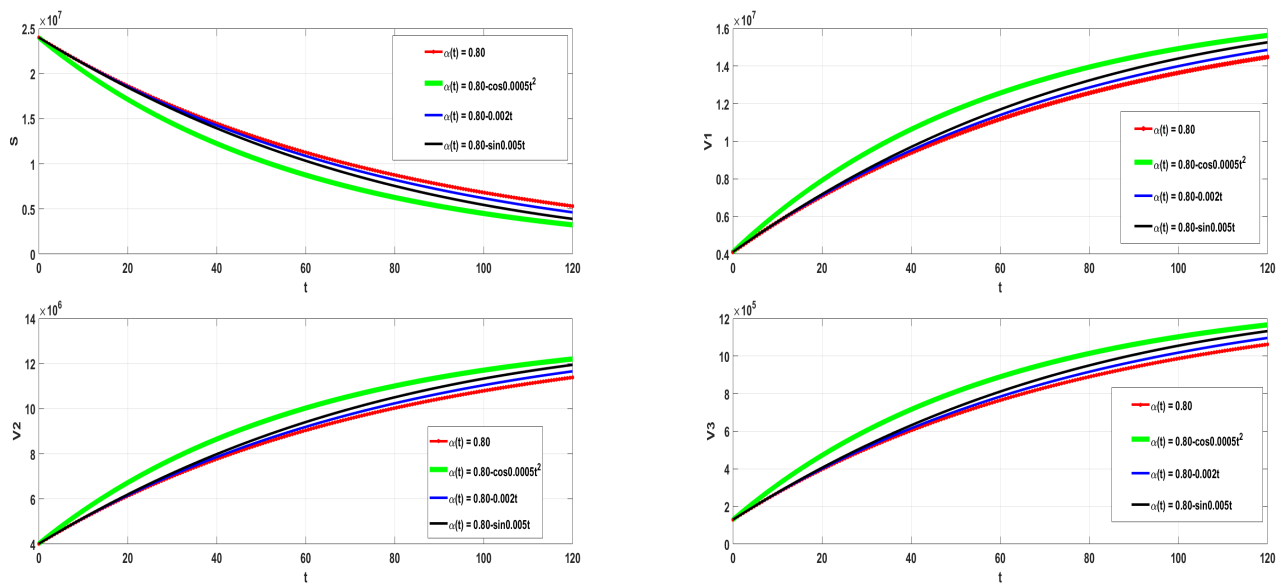


Figure 3. The solution behavior using the method in [24] with different values of $\alpha(t)$.

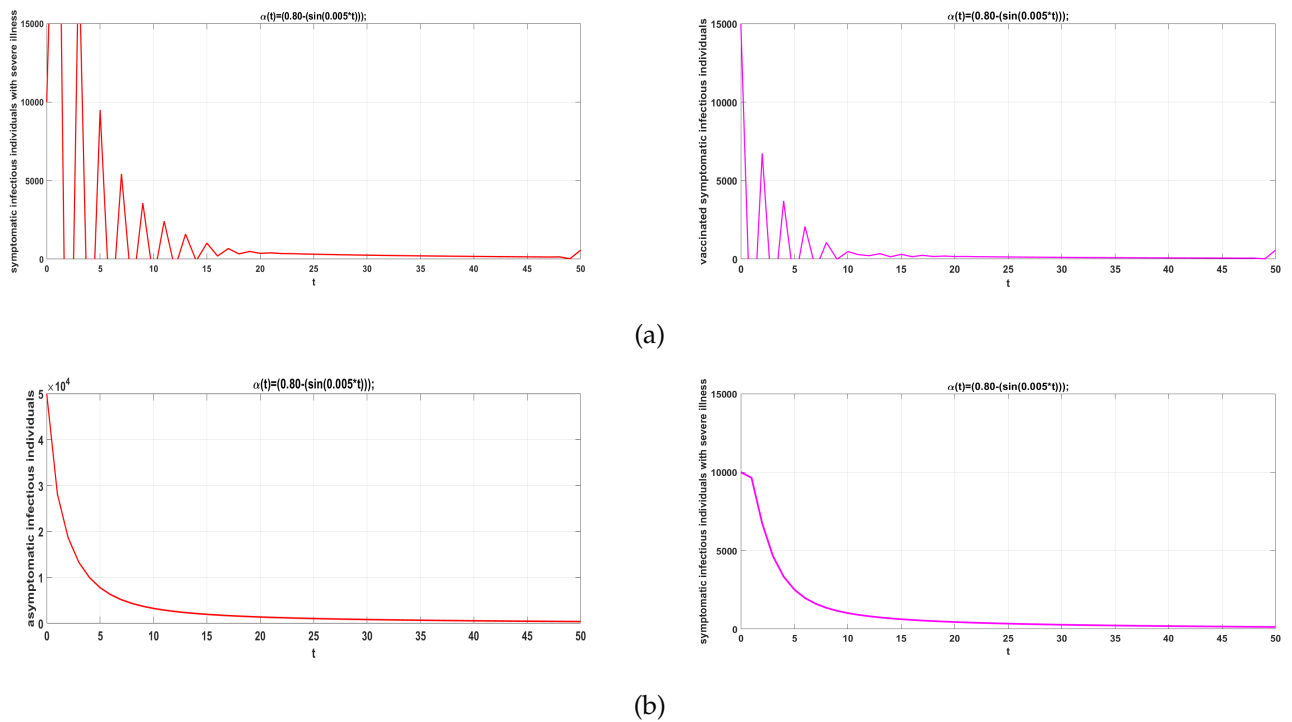


Figure 4. The solution behavior using the method [24] in (a) and using CPC- Θ FDM and $\Theta = 0$, in (b).

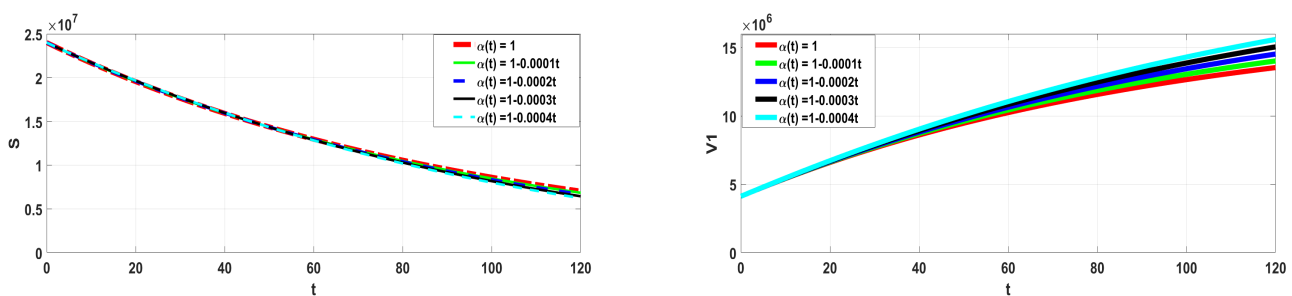


Figure 5. Cont.

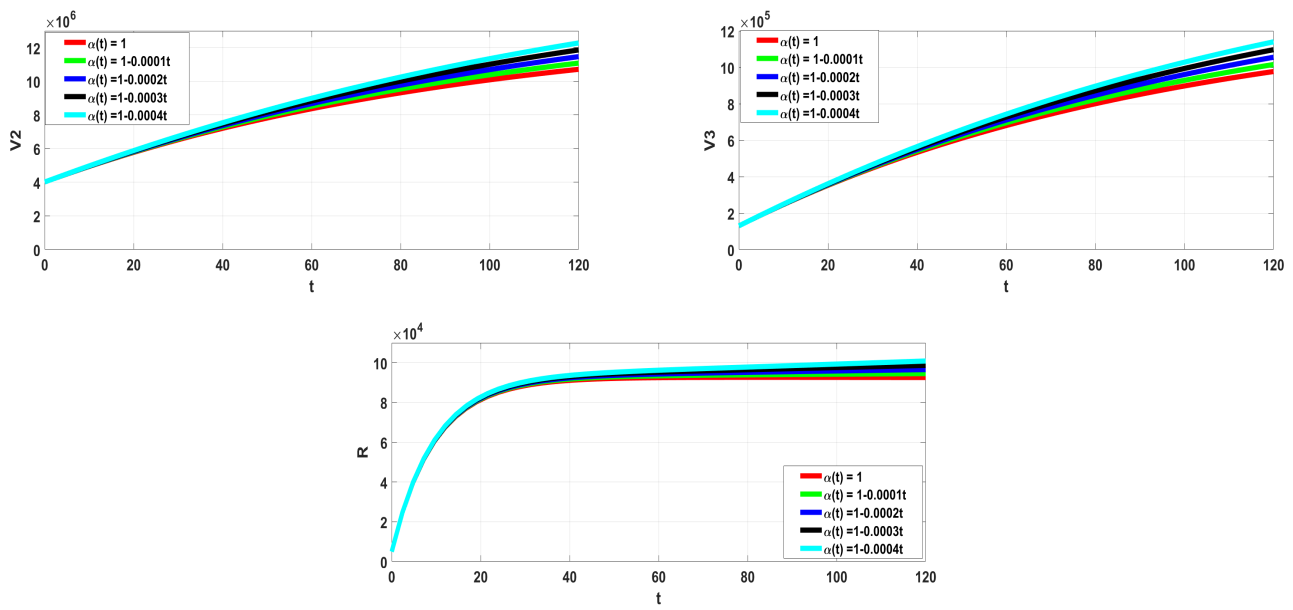


Figure 5. The solution behavior acquired via CPC- Θ FDM and $\Theta = 0.5$, of (8).

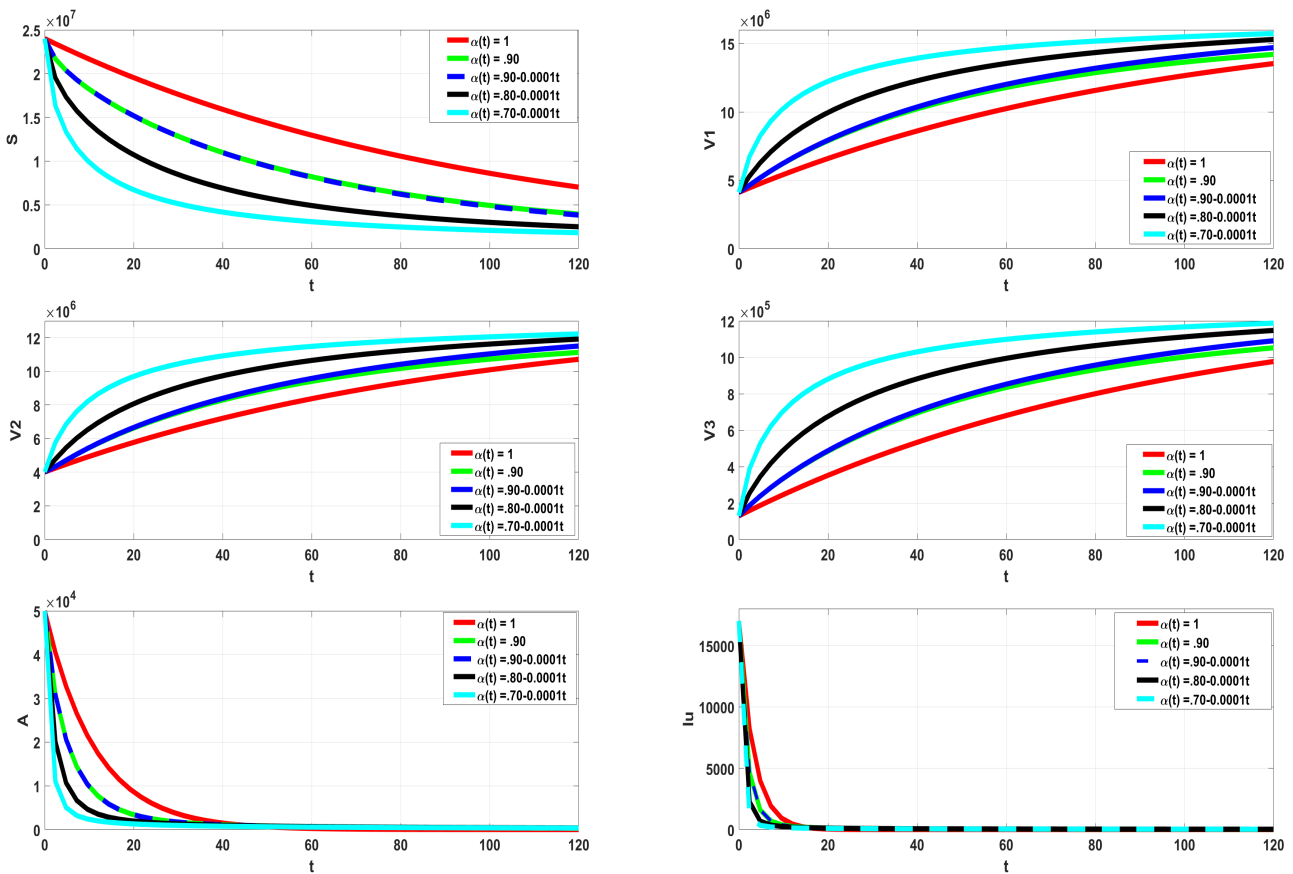


Figure 6. Cont.

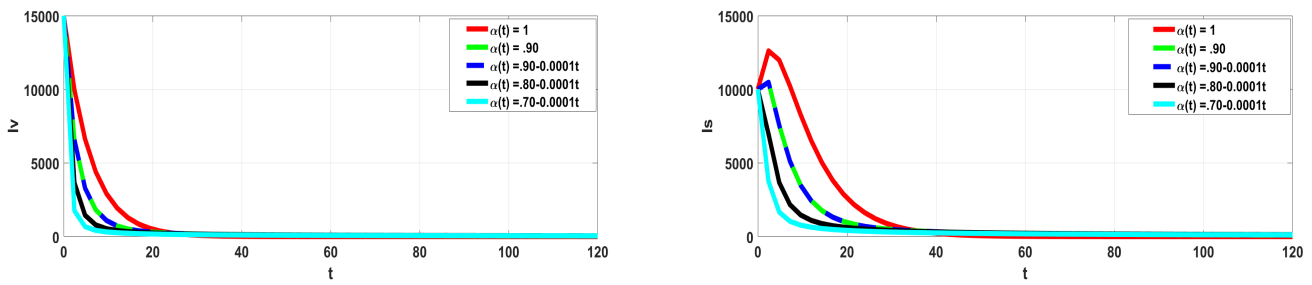


Figure 6. The solution behavior acquired via CPC- Θ FDM and $\Theta = 1$ of (8).

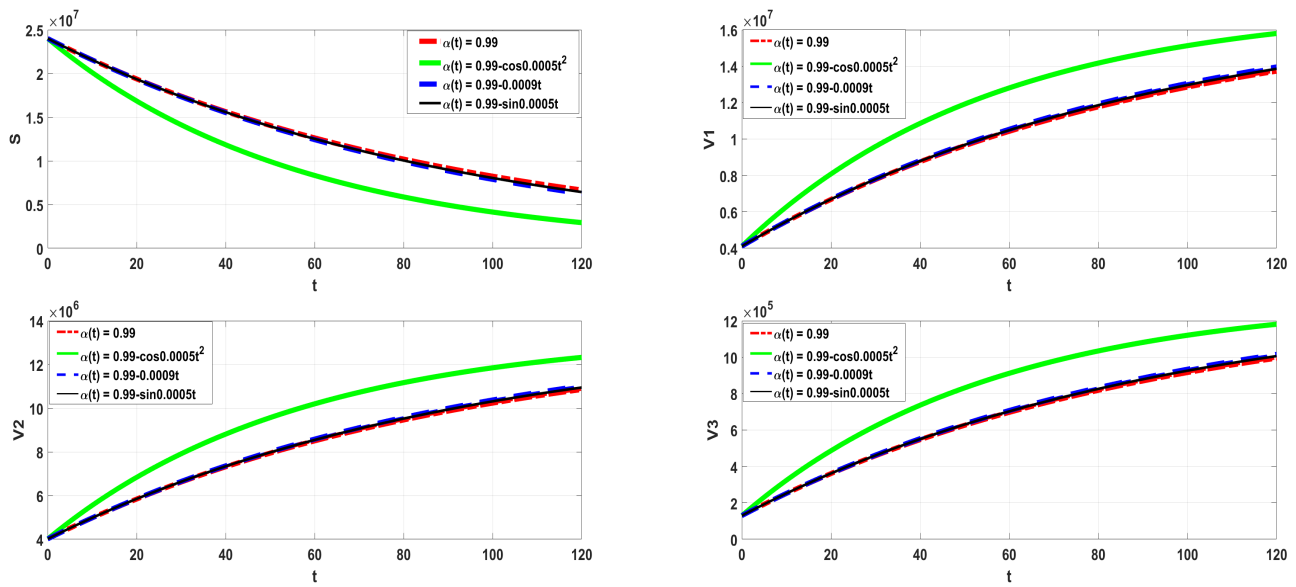


Figure 7. The solution behavior acquired via GRK4M of (8).

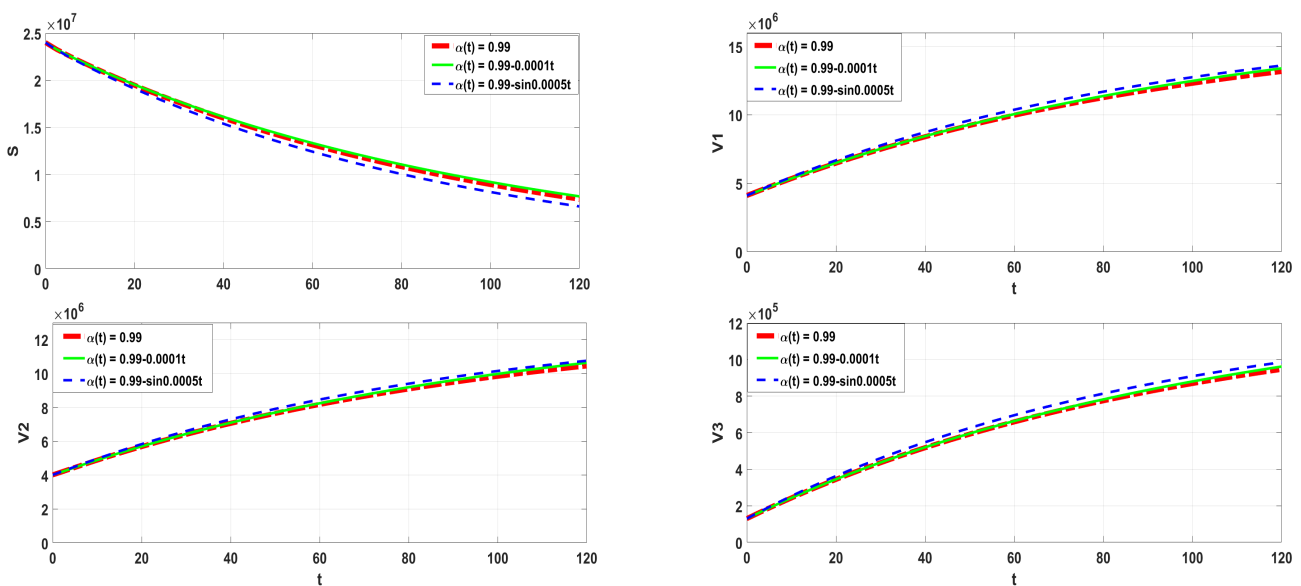


Figure 8. The solution behavior acquired via CPC- Θ FDM and $\Theta = 0$ of (8).

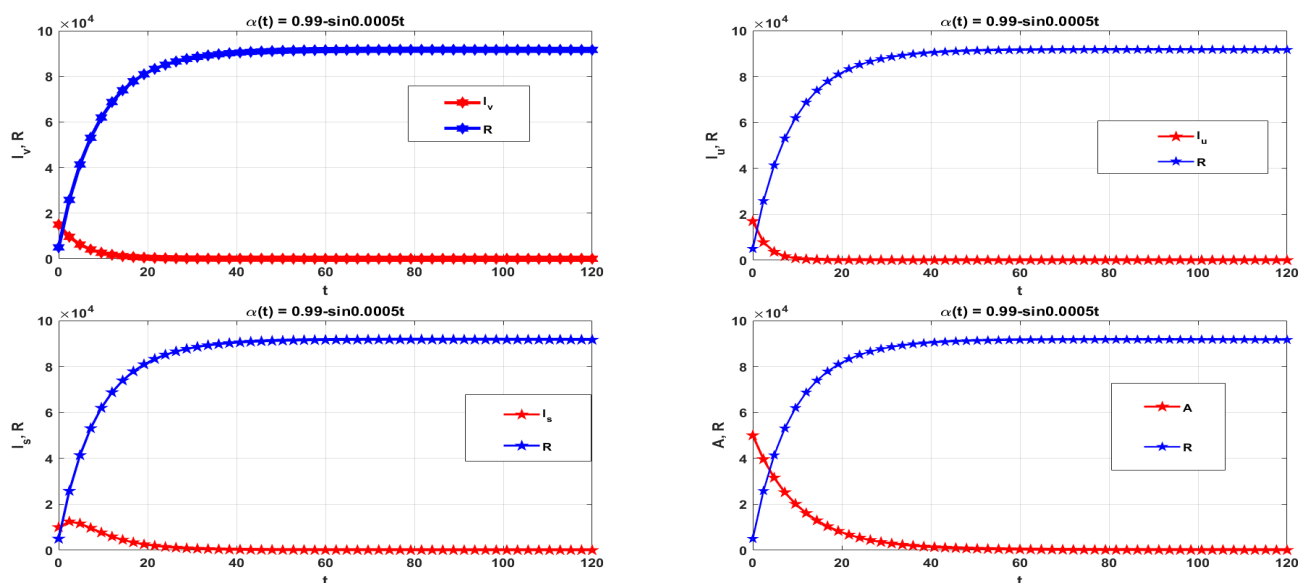


Figure 9. The relation between the variables concerning nonlinear $\alpha(t)$ using CPC- Θ FDM and $\Theta = 0$.

6. Conclusions

A novel hybrid variable-order fractional multi-vaccination model for COVID-19 is presented in this paper in order to further explore the spread of COVID-19. The main advantage of the hybrid variable-order fractional operator is that it can be defined as a linear combination of the variable-order integral of Riemann–Liouville and the variable-order Caputo derivative; it is one of the most effective and reliable operators and it is more general than the Caputo fractional operator. The proposed model's dynamics are improved and its complexity is increased by employing variable-order fractional derivatives. Furthermore, the variable-order fractional Caputo operator can be derived as a special case from the CPC operator. Existence, boundedness, uniqueness, positivity and stability of the proposed model are established for the model. To be compatible with the physical model, a new parameter σ is added. The proposed model is numerically studied using CPC- Θ FDM and GRK4M. CPC- Θ FDM depends on the values of the factor Θ . It can be explicit ($\Theta = 1$) or fully implicit ($\Theta = 0$) with a large stability region. We compared our results with the real data from the state of Texas in the United States. Moreover, the results obtained from the CPC- Θ FDM are more stable than the results obtained from the proposed method in [24]. As a result, some graphs are provided for various linear and non-linear variable-order derivatives. In the future, the presented study can be extended to optimal control and to examine the impact of multiple vaccination strategies on the dynamics of COVID-19 in a population.

Author Contributions: Conceptualization, T.A.A.; Methodology, N.S. and S.M.A.-M.; Software, S.M.A.-M. and R.G.S.; Formal analysis, N.S.; Investigation, R.G.S. and T.A.A.; Resources, S.M.A.-M.; Writing—original draft, T.A.A.; Writing—review and editing, N.S. and R.G.S. All authors have read and agreed to the published version of the manuscript.

Funding: This research received no external funding.

Data Availability Statement: Not applicable.

Conflicts of Interest: The authors declare no conflict of interest.

References

1. United States Food and Drug Administration. FDA Takes Key Action in Fight Against COVID-19 By Issuing Emergency Use Authorization for First COVID-19 Vaccine. 2020. Available online: <https://www.fda.gov/news-events/press-announcements/fda-takes-key-action-fight-against-COVID-19-issuing-emergency-use-authorization-first-COVID-19> (accessed on 17 June 2021).
2. Interim Clinical Considerations for Use of COVID-19 Vaccines Currently Authorized in the United States. Available online: <https://www.cdc.gov/vaccines/COVID-19/clinical-considerations/COVID-19-vaccines-us.html> (accessed on 14 July 2021).
3. Machado, J.A.T.; Lope, A.M. Rare and extreme events: The case of COVID-19 pandemic. *Nonlinear Dyn.* **2020**, *100*, 2953–2972. [CrossRef] [PubMed]
4. Bonyah, E.; Sagoe, A.K.; Kumar, D.; Deniz, S. Fractional optimal control dynamics of Coronavirus model with Mittag-Leffler law. *Ecol. Complex.* **2020**, *45*, 100880. [CrossRef]
5. Ali, A.; Alshammari, F.S.; Islam, S.; Khan, M.A.; Ullah, S. Modeling and analysis of the dynamics of novel coronavirus (COVID-19) with Caputo fractional derivative. *Results Phys.* **2020**, *20*, 103669. [CrossRef] [PubMed]
6. Danane, J.; Hammouch, Z.; Allali, K.; Rashid, S.; Singh, J. A fractional-order model of coronavirus disease 2019 (COVID-19) with governmental action and individual reaction. *Math. Meth. Appl. Sci.* **2021**, 1–14. [CrossRef]
7. Yadav, S.; Kumar, D.; Singh, J.; Baleanu, D. Analysis and dynamics of fractional order COVID-19 model with memory effect. *Results Phys.* **2021**, *24*, 104017. [CrossRef]
8. Sinan, M.; Ali, A.; Shah, K.; Assiri, T.; Nofal, T.A. Stability analysis and optimal control of COVID-19 pandemic SEIQR fractional mathematical model with harmonic mean type incidence rate and treatment. *Results Phys.* **2021**, *22*, 103873. [CrossRef]
9. Conejero, J.A.; Franceschi, J.; Picó-Marco, E. Fractional vs. Ordinary Control Systems: What Does the Fractional Derivative Provide? *Mathematics* **2022**, *10*, 2719. [CrossRef]
10. Samko, S.G.; Ross, B. Integration and differentiation to a variable fractional order. *Integral Transform. Spec. Funct.* **1993**, *1*, 277–300. [CrossRef]
11. Solís-Pérez, J.E.; Gómez-Aguilar, J.F. Novel numerical method for solving variable-order fractional differential equations with power, exponential and Mittag-Leffler laws. *Chaos Solitons Fractals* **2018**, *14*, 175–185. [CrossRef]
12. Sun, H.; Chang, A.; Zhang, Y.; Chen, W. A review on variable-order fractional differential equations: Mathematical foundations, physical models and its applications. *Fract. Calc. Appl. Anal.* **2019**, *22*, 27–59. [CrossRef]
13. Sweilam, N.H.; Al-Mekhlafi, S.M. Numerical study for multi-strain tuberculosis (TB) model of variable-order fractional derivatives. *J. Adv. Res.* **2016**, *7*, 271–283. [CrossRef]
14. Sweilam, N.H.; L-Mekhlafi, S.M.A.; Shatta, S.A.; Baleanu, D. Numerical study for two types variable-order Burgers' equations with proportional delay. *Appl. Numer. Math.* **2020**, *156*, 364–376. [CrossRef]
15. Sweilam, N.H.; Assiri, T.; Hasan, M.A. Numerical solutions of nonlinear fractional Schrödinger equations using nonstandard discretizations, Numerical Solutions of Nonlinear Fractional Schrödinger Equations. *Numer. Methods Partial. Differ. Equ.* **2017**, *33*, 1399–1419. [CrossRef]
16. Sweilam, N.H.; Assiri, T. Numerical scheme for solving the space-time variable order nonlinear fractional wave equation. *Prog. Fract. Differ. Appl.* **2015**, *1*, 269–280. [CrossRef]
17. Bha, I.A.; Mishra, L.N. Numerical solutions of Volterra integral equations of third kind and its convergence analysis. *Symmetry* **2022**, *14*, 2600.
18. Pathak, V.K.; Mishra, L.N. Application of Fixed point theorem to solvability for non-linear fractional Hadamard functional integral equations. *Mathematics* **2022**, *10*, 2400. [CrossRef]
19. Smith, G.D. Numerical solution of partial differential equations: Finite difference methods. In *Oxford Applied Mathematics and Computing Science Series*; Oxford University Press: Oxford, UK, 1985.
20. Yuste, S.B. Weighted average finite difference methods for fractional diffusion equations. *J. Comput. Phys.* **2006**, *216*, 264–274. [CrossRef]
21. Sweilam, N.H.; Hasan, M.M.A. An Improved method for nonlinear variable-order Lévy-Feller advection-dispersion equation. *Bull. Malays. Math. Sci. Soc.* **2019**, *42*, 3021–3046. [CrossRef]
22. Sweilam, N.H.; Hasan, M.M.A.; Al-Mekhlafi, S.M.; Al khatib, S. Time fractional of nonlinear heat-wave propagation in a rigid thermal conductor: Numerical treatment. *AEJ—Alex. Eng. J.* **2022**, *61*, 10153–10159. [CrossRef]
23. Milici, C.; Machado, J.T.; Draganescu, G. Application of the Euler and Runge–Kutta generalized methods for FDE and symbolic packages in the analysis of some fractional attractors. *Int. J. Nonlinear Sci. Numer. Simul.* **2020**, *21*, 159–170. [CrossRef]
24. Oname, A.; Okuonghae, D.; Nwajeri, U.K.; Onyenegecha, C.P. A fractional-order multi-vaccination model for COVID-19 with non-singular kernel. *Alex. Eng. J.* **2022**, *16*, 6089–6104. [CrossRef]
25. Sun, H.G.; Chen, W.; Wei, H.; Chen, Y.Q. A comparative study of constant-order and variable-order fractional models in characterizing memory property of systems. *Eur. Phys. J. Spec. Top.* **2011**, *193*, 185–192. [CrossRef]
26. Baleanu, D.; Fernandez, A.; Akgül, A. On a fractional operator combining proportional and classical differintegrals. *Mathematics* **2020**, *8*, 360. [CrossRef]
27. Ullah, M.Z.; Baleanu, D. A new fractional SICA model and numerical method for the transmission of HIV / AIDS. *Math. Meth. Appl. Sci.* **2021**, *44*, 4648–4659. [CrossRef]
28. Lin, W. Global existence theory and chaos control of fractional differential equations. *J. Math. Anal. Appl.* **2007**, *332*, 709–726. [CrossRef]

29. Texas Population, Census Reporter. Available online: <https://censusreporter.org/profiles/04000US48-texas/> (accessed on 26 June 2021).
30. United States Food and Drug Administration. FDA Briefing Document Moderna COVID-19 Vaccine. 2020. Available online: <https://www.fda.gov/media/144434/download> (accessed on 17 June 2021).
31. United States Food and Drug Administration. FDA Briefing Document Pfizer-BioNTech COVID-19 Vaccine. 2020. Available online: <https://www.fda.gov/media/144245/download> (accessed on 17 June 2021).
32. Okuonghae, D.; Omame, A. Analysis of a mathematical model for COVID-19 population dynamics in Lagos, Nigeria. *Chaos Solitons Fractals* **2020**, *139*, 110032. [[CrossRef](#)]
33. Chu, Y.-M.; Yassen, M.F.; Ahmad, I.; Sunthrayuth, P.; Khan, M.A. A fractional SARS-COV-2 model with Atangana-Baleanu derivative: Application to fourth wave. *Fractals* **2022**, *30*, 2240210. . [[CrossRef](#)]
34. Driessche, P.; Watmough, P. Reproduction numbers and sub-threshold endemic equilibria for compartmental models of disease transmission. *Math. Biosci.* **2002**, *180*, 29–48. [[CrossRef](#)]
35. Fosu, G.O.; Akweitley, E. Albert-adu-sackey, Next-generation matrices and basic reproductive numbers for all phases of the Coronavirus disease. *Open J. Math. Sci.* **2020**, *4*, 261–272. [[CrossRef](#)]
36. Sekerci, Y. Climate change forces plankton species to move to get rid of extinction: Mathematical modeling approach. *Eur. Phys. J. Plus* **2020**, *135*, 794. [[CrossRef](#)]
37. Al-Mekhlafi, S.M.; Sweilam, N.H. *Numerical Studies for Some Tuberculosis Models*; LAP LAMBERT Academic Publishing: London, UK, 2016; 156p.
38. Sweilam, N.H.; L-Mekhlafi, S.M.A.; Alshomrani, A.S.; Baleanu, D. Comparative study for optimal control nonlinear variable-order fractional tumor model. *Chaos Solitons Fractals* **2020**, *136*, 109810. [[CrossRef](#)]
39. Scherer, R.; Kalla, S.; Tang, Y.; Huang, J. The Grünwald-Letnikov method for fractional differential equations. *Comput. Math. Appl.* **2011**, *62*, 902–917. [[CrossRef](#)]
40. Arenas, A.J.; González-Parra, G.; Chen-Charpentier, B.M. Construction of nonstandard finite difference schemes for the SI and SIR epidemic models of fractional order. *Math. Comput. Simul.* **2016**, *121*, 48–63. [[CrossRef](#)]
41. Yuste, S.B.; Quintana-Murillo, J. A finite difference method with non-uniform time steps for fractional diffusion equations. *Comput. Phys. Commun.* **2012**, *183*, 2594–2600. [[CrossRef](#)]
42. COVID-19 Vaccinations in the US. Available online: <https://data.cdc.gov/Vaccinations/COVID-19-Vaccinations-in-the-United-States-Jurisdi/uns> (accessed on 13 March 2021).

Disclaimer/Publisher’s Note: The statements, opinions and data contained in all publications are solely those of the individual author(s) and contributor(s) and not of MDPI and/or the editor(s). MDPI and/or the editor(s) disclaim responsibility for any injury to people or property resulting from any ideas, methods, instructions or products referred to in the content.